

Supporting Information

Enhanced Photocatalytic and Antibacterial Ability of Cu-doped Anatase TiO₂ Thin Films: Theory and Experiment

Abdullah M. Alotaibi^{a,b}, Benjamin A. D. Williamson^{c,d}, Sanjayan Sathasivam^a,
Andreas Kafizas^e, Mahdi Alqahtani^{f,g}, Carlos Sotelo-Vazquez^a, John Buckeridge^h,
Jiang Wu^{f,i}, Sean P. Nair^j, David O. Scanlon^{c,d,k*} and Ivan P. Parkin^{a*}

**Corresponding authors*

(a) Materials Chemistry Centre, Department of Chemistry, University College London, 20 Gordon Street, London WC1H 0AJ, UK

(b) The National Centre for Building and Construction Technology, King Abdulaziz City for Science and Technology (KACST), Riyadh, 11442-6086, Saudi Arabia

(c) Department of Chemistry, Christopher Ingold Building, University College London, 20 Gordon Street, London WC1H 0AJ, UK.

(d) Thomas Young Centre, University College London, Gower Street, London WC1E 6BT, United Kingdom.

(e) Grantham Institute, Imperial College London, Exhibition Road, London, SW7 2AZ, UK

(f) Electronic & Electrical Engineering, University College London, Torrington Place, London, UK WC1E 7JE

(g) Materials Science Research Institute King Abdulaziz City for Science and Technology (KACST), Riyadh, 11442-6086, Saudi Arabia

(h) School of Engineering, London South Bank University, 103 Borough Road, London SE1 0AA, UK

(i) University of Electronic Science and Technology of China, North Jianshe Road, Chengdu, 610054, China

(j) Department of Microbial Diseases, UCL Eastman Dental Institute, 256 Gray's Inn Road, London, WC1X 8LD

(k) Diamond Light Source Ltd., Diamond House, Harwell Science and Innovation Campus, Didcot, Oxfordshire OX11 0DE, United Kingdom.

* Fax: (+44) 20-7679-7463

* E-mail: d.scanlon@ucl.ac.uk ; i.p.parkin@ucl.ac.uk

Defect Formalism

For a defect (D) in charge state q the formation enthalpy, $\Delta H_f(D, q)$, can be defined as:

$$\Delta H_f(D, q) = (E^{D,q} - E^H) + \sum_i n(E_i + \mu_i) + q(E_{Fermi} + \varepsilon_{VBM}^H + \Delta E_{pot}) + q^2 E_{corr}^{IC} + E_{corr}^{BF} \quad (1)$$

$E^{D,q}$ and E^H are the total energies of the defective supercell (in charge state ' q ') and the host supercell respectively. A relation to the elemental chemical potentials is represented by μ_i (where E_i is the elemental reference energy and ' i ' refers to the species involved: $Ti_{(s)}$, $O_{2(g)}$, and $Cu_{(s)}$). n is either positive or negative dependent on whether the species is removed ($+n$) or added ($-n$) to the system. The Fermi level (E_f) ranges from the valence band maximum (VBM) to the conduction band minimum (CBM) in this work which is determined to be 3.35eV above the VBM consistent with other *ab-initio* works.¹⁻⁸ ε_{VBM}^H is the eigenvalue of the VBM of the host supercell and ΔE_{pot} is a potential alignment term which is a correction applied to account for the difference between the potential of the defective and host supercells. Lastly two corrections must be applied to account for the finite size of the supercells: an image charge correction, $q^2 E_{corr}^{IC}$, and a band filling correction, E_{corr}^{BF} (for shallow defects). $q^2 E_{corr}^{IC}$ is necessary due to the long-ranged nature of the Coulomb interaction⁹⁻¹⁰ and thus the interaction of the charged defect and its periodic images. The scheme used herein is based on a formalism created by Hine and Murphy¹¹. The *band filling* correction created by Lany and Zunger¹²⁻¹³ accounts for the high defect concentrations giving rise to unphysical band gap renormalisation errors present in supercell calculations.

Thermodynamic Limits

To determine the formation enthalpies of each defect a chemical potential range is created representing the equilibrium growth conditions within the bounds of the formation of $O_{2(g)}$ and the secondary phase of Ti_2O_3 under *Ti-poor/O-rich* and *Ti-rich/O-poor* respectively. Therefore: we can define the chemical potentials under *Ti-poor/O-rich* to be:

$$\mu_{Ti} + 2\mu_O = \Delta H_f^{TiO_2} = -9.14 \text{ eV} \quad (2)$$

Where under the formation of $O_{2(g)}$ gives the chemical potentials:

$$\mu_O = 0 \text{ eV and } \mu_{Ti} = -9.14 \text{ eV} \quad (3)$$

At the *Ti-rich/O-poor* boundary, the chemical potentials are limited by the formation of Ti_2O_3 therefore:

$$2\mu_{Ti} + 3\mu_O = \Delta H_f^{Ti_2O_3} = -14.76 \text{ eV} \quad (4)$$

Then

$$\mu_O = -2.11 \text{ eV and } \mu_{Ti} = -3.51 \text{ eV} \quad (5)$$

A further constraint is placed on the dopant species and is limited by the formation of CuO:

$$\mu_{Cu} + \mu_O = \Delta H_f^{CuO} = -1.45 \text{ eV} \quad (6)$$

μ_{Cu} is therefore -1.45 eV under *Ti-poor/O-rich* conditions and under *Ti-rich/O-poor* conditions μ_{Cu} is limited by the formation of Cu-metal, therefore $\mu_{Cu} = 0 \text{ eV}$.

The thermodynamic transition levels are displayed in **Figure 1** and display the change of a defect from charge state q to q' at a specific Fermi energy and is calculated using the equation:

$$\varepsilon(q/q') = \frac{\Delta H_f(D,q) - \Delta H_f(D,q')}{q' - q} \quad (7)$$

These transition levels can be observed using techniques such as deep level transient spectroscopy, DLTS.

Optical Absorption and Emission

Optical absorption and emission energies can be evaluated for a given defect. These involve the excitation of an electron from a defect level to the conduction band minimum (E_{abs}) and then the subsequent recapture of an electron (E_{em}). Alternatively a similar analysis can be carried out on hole capture from the valence band.¹⁴⁻¹⁵ These processes can be matched experimentally through optical transmission and photoluminescence measurements, an approach that has been successfully applied to a range of defects and materials.¹⁴⁻¹⁸ The construction of a “configurational coordinate” diagram is typically carried out to depict these processes as shown in Figure 9. The underlying assumption in evaluating the optical transitions is that photoexcitation occurs on a much faster timescale to that of lattice relaxation, as per the Franck-Condon principle¹⁹⁻²⁰. Therefore to calculate these optical processes the unrelaxed excited state (post-absorption) is calculated within the relaxed equilibrium geometry of the ground state, and vice versa for the emission process.¹⁶⁻¹⁷ The eventual lattice relaxation leads to a release in energy (E_{rel}) via the emission of phonons. The difference between the equilibrium geometries of the ground and excited states corresponds to the zero-phonon line or the *thermal transition level*, $\varepsilon(q/q')$. The generalised coordinate was calculated by evaluating the mean displacement of atoms in the supercell above a suitable

threshold ($>0.01 \text{ \AA}$ displacement) between the equilibrium configurations of the different charge states.

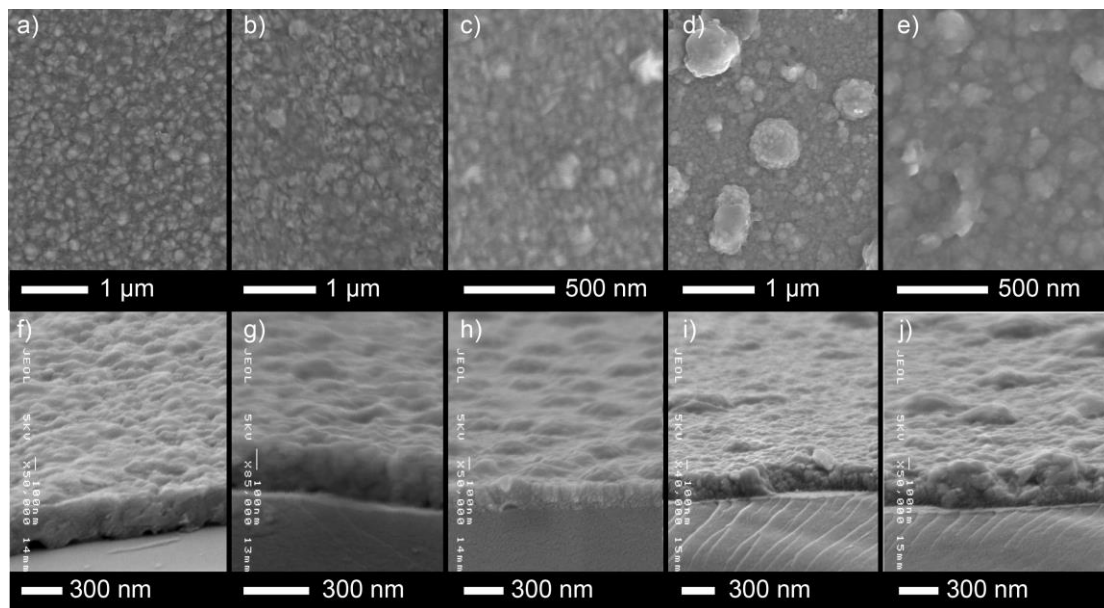


Figure S1: Top down SEM images of the **a)** 0%, **b)** 2%, **c)** 5%, **d)** 10% and **e)** 20% Cu doped TiO_2 as well as side-on images of **f)** 0%, **g)** 2%, **h)** 5%, **i)** 10% and **j)** 20% Cu doped TiO_2 films grown via AACVD from $[\text{Ti}(\text{OCH}(\text{CH}_3)_2)_4]$ and $[\text{Cu}(\text{NO}_3)_2 \cdot 3\text{H}_2\text{O}]$. The side-on SEM images also presented show the thickness of the films.

Figure 1S shows the top down and side on scanning electron microscopy (SEM) images for TiO_2 thin films of various Cu concentration. The pure TiO_2 (**Figure 1a**), 2% and 5% doped TiO_2 :Cu films have very similar morphology consisting of densely packed particles *ca.* 150 nm wide with no signs of pin holes, voids or cracks. All films were *ca.* 300 nm thick. At the higher doping levels (10% and 20%), large globular features are present.

1. Heyd, J.; Scuseria, G. E.; Ernzerhof, M., Hybrid Functionals Based on a Screened Coulomb Potential. *The Journal of chemical physics* **2003**, *118* (18), 8207-8215.
2. Scanlon, D. O.; Morgan, B. J.; Watson, G. W., Modeling the Polaronic Nature of P-Type Defects in Cu 2 O: The Failure of Gga and Gga+ U. *The Journal of chemical physics* **2009**, *131* (12), 124703.
3. Landmann, M.; Rauls, E.; Schmidt, W., The Electronic Structure and Optical Response of Rutile, Anatase and Brookite TiO_2 . *Journal of physics: condensed matter* **2012**, *24* (19), 195503.

4. Dou, M.; Persson, C., Comparative Study of Rutile and Anatase SnO₂ and TiO₂: Band-Edge Structures, Dielectric Functions, and Polaron Effects. *Journal of Applied Physics* **2013**, *113* (8), 083703.
5. Patrick, C. E.; Giustino, F., Gw Quasiparticle Bandgaps of Anatase TiO₂ Starting from DFT+U. *Journal of Physics: Condensed Matter* **2012**, *24* (20), 202201.
6. Kang, W.; Hybertsen, M. S., Quasiparticle and Optical Properties of Rutile and Anatase TiO₂. *Physical Review B* **2010**, *82* (8), 085203.
7. Sai, G.; Bang-Gui, L., Electronic Structures and Optical Properties of TiO₂: Improved Density-Functional-Theory Investigation. *Chinese Physics B* **2012**, *21* (5), 057104.
8. Buckeridge, J.; Butler, K. T.; Catlow, C. R. A.; Logsdail, A. J.; Scanlon, D. O.; Shevlin, S. A.; Woodley, S. M.; Sokol, A. A.; Walsh, A., Polymorph Engineering of TiO₂: Demonstrating How Absolute Reference Potentials Are Determined by Local Coordination. *Chemistry of Materials* **2015**, *27* (11), 3844-3851.
9. Hine, N.; Frensch, K.; Foulkes, W.; Finnis, M., Supercell Size Scaling of Density Functional Theory Formation Energies of Charged Defects. *Physical Review B* **2009**, *79* (2), 024112.
10. Nieminen, R. M., Issues in First-Principles Calculations for Defects in Semiconductors and Oxides. *Modelling and Simulation in Materials Science and Engineering* **2009**, *17* (8), 084001.
11. Murphy, S. T.; Hine, N. D., Anisotropic Charge Screening and Supercell Size Convergence of Defect Formation Energies. *Physical Review B* **2013**, *87* (9), 094111.
12. Lany, S.; Zunger, A., Assessment of Correction Methods for the Band-Gap Problem and for Finite-Size Effects in Supercell Defect Calculations: Case Studies for ZnO and GaAs. *Physical Review B* **2008**, *78* (23), 235104.
13. Freysoldt, C.; Neugebauer, J.; Van de Walle, C. G., Fully Ab Initio Finite-Size Corrections for Charged-Defect Supercell Calculations. *Physical Review Letters* **2009**, *102* (1), 016402.
14. Frodason, Y.; Johansen, K.; Bjørheim, T.; Svensson, B.; Alkauskas, A., Zn Vacancy as a Polaronic Hole Trap in ZnO. *Physical Review B* **2017**, *95* (9), 094105.
15. Lyons, J. L.; Alkauskas, A.; Janotti, A.; Van de Walle, C. G., First - Principles Theory of Acceptors in Nitride Semiconductors. *physica status solidi (b)* **2015**, *252* (5), 900-908.
16. Van de Walle, C. G.; Neugebauer, J., First-Principles Calculations for Defects and Impurities: Applications to III-Nitrides. *Journal of applied physics* **2004**, *95* (8), 3851-3879.
17. Alkauskas, A.; McCluskey, M. D.; Van de Walle, C. G., Tutorial: Defects in Semiconductors—Combining Experiment and Theory. *Journal of Applied Physics* **2016**, *119* (18), 181101.
18. Varley, J.; Janotti, A.; Van de Walle, C., Mechanism of Visible - Light Photocatalysis in Nitrogen - Doped TiO₂. *Advanced Materials* **2011**, *23* (20), 2343-2347.
19. Franck, J.; Dymond, E., Elementary Processes of Photochemical Reactions. *Transactions of the Faraday Society* **1926**, *21* (February), 536-542.
20. Condon, E., A Theory of Intensity Distribution in Band Systems. *Physical Review* **1926**, *28* (6), 1182.